Section 7

Global and regional climate models, sensitivity and impact experiments, response to external forcing, monthly and seasonal forecasting.

Estimates of changes in soil thermal regime and methane emissions in the northern regions of Western Siberia in the 21st century

Maxim M Arzhanov, Sergey N Denisov

A.M. Obukhov Institute of Atmospheric Physics, RAS, Moscow, Russia
arzhanov@ifaran.ru

According to observational data, climate warming in the western sector of the Russian Arctic since 1970 is characterized by an increase in the surface temperature of the atmosphere and the duration of the warm period, a change in the amount of precipitation, and an increase in the thickness of the snow cover. Due to regional climatic changes over the last 40-50 years, the temperature of permafrost in the northern regions of Western Siberia has increased with the growth of the seasonally thawed layer thickness [Streletskiy et al., 2015; Biskaborn et al., 2019].

Estimates of possible changes in the thermal state of the cryolithozone, obtained using equilibrium and dynamic ground heat transfer models, which differ in the degree of detail of the processes described, also show that in the next 50-100 years, the dynamics of the permafrost temperature increase may persist, leading to a reduction in the permafrost spread area due to partial or complete permafrost degradation in some regions [Nicolsky et al., 2018].

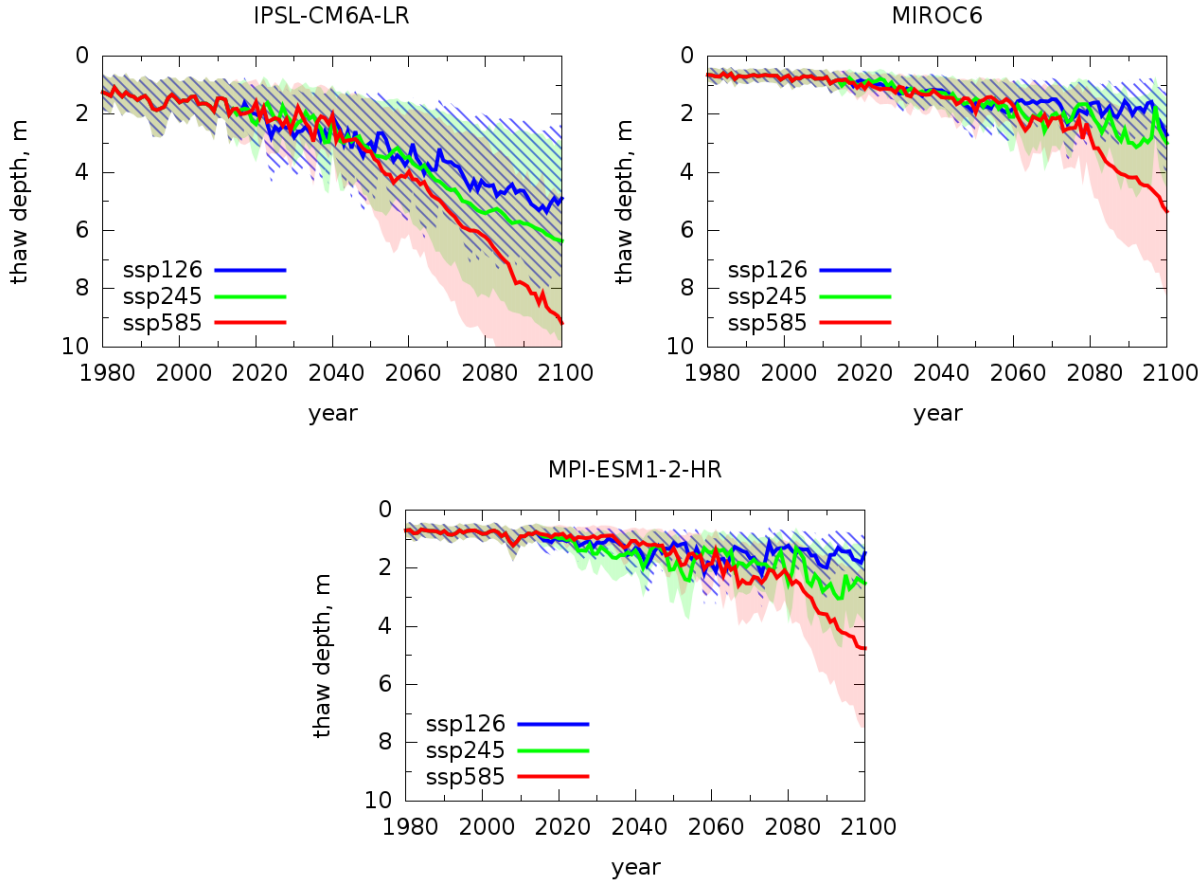

Figure 1. Model estimates of interannual changes in maximum seasonal thaw depth (m) in Western Siberia.

Using a one-dimensional model of heat transfer in soils, developed for the IAP RAS climate model, the depth of seasonal thawing in northern Siberia was calculated (Fig. 1). As input data (temperature, precipitation) the results of calculations with global climate models of

the CMIP6 project (IPSL-CM6A-LR, MIROC6, MPI-ESM1-2-HR) under three scenarios of anthropogenic forcing (ssp1-26, ssp2-45, ssp5-85) were used. The results obtained show that in the coming decades, the continuing growth of the near-surface temperature will lead to an increase in the maximum depth of seasonal thawing in the northern regions of Siberia.

Methane emissions from wetlands were estimated using the IAP RAS methane cycle model. Contemporary annual emissions from Western Siberia equal to 3.8 TgCH4 with more than 2 TgCH4 emitted in the second half of warm period (i.e., August-September) when the thaw depth is largest and the soil temperature is highest. As the surface temperature increases and the warm period lengthens, demonstrating most pronounced effects in the high latitudes of the northern hemisphere, methane emissions increase rapidly. According to estimates, in the northern regions of Western Siberia, under the most unfavorable scenarios in the 21st century, their growth may reach up to 600-700%. It is also worth considering possible variations in emission due to changes in the soil moisture regime.

This work was supported by the Russian Science Foundation (project 19-17-00240).

Biskaborn B.K., Lanckman J.-P., Lantuit H. et al. The new database of the Global Terrestrial Network for Permafrost (GTN-P) // Earth Syst. Sci. Data. 2015. No. 67. P. 245–259.

Biskaborn B.K., Smith S.L., Noetz L.J. et al. Permafrost is warming at a global scale // Nature Communications. 2019. Vol. 10. P. 264.

Nicolsky D.J., Romanovsky V.E. Modeling long-term permafrost degradation // J. Geophys. Res. 2018. Vol. 123. P. 1-15.

Streletskiy D., Anisimov O., Vasiliev A. Permafrost degradation / Snow and Ice-Related Hazards, Risks and Disasters. New York: Elsevier. 2015. P. 303–344.

Estimates of contemporary natural carbon dioxide fluxes in Russia and their uncertainties based on CMIP6 ensemble data

Sergey N Denisov, Igor I Mokhov

A.M. Obukhov Institute of Atmospheric Physics, RAS, Moscow, Russia
denisov@ifaran.ru

A detailed and comprehensive analysis of the impact of changes in the carbon cycle in the Earth's climate system requires, among other things, adequate consideration of the carbon balance of boreal forests, wetlands and other ecosystems. It has previously been shown that natural carbon dioxide fluxes on the territory of Russia can change significantly at the scale of decades in model experiments [1], which can lead to changes in the role of natural terrestrial ecosystems in global climate change.

To understand the ability of current global climate models to adequately reproduce natural carbon dioxide fluxes we analyzed data from global climate models of the CMIP6 project, designed for multi-model assessments. Such multi-model results can provide some perspective on errors and uncertainty in model simulations.

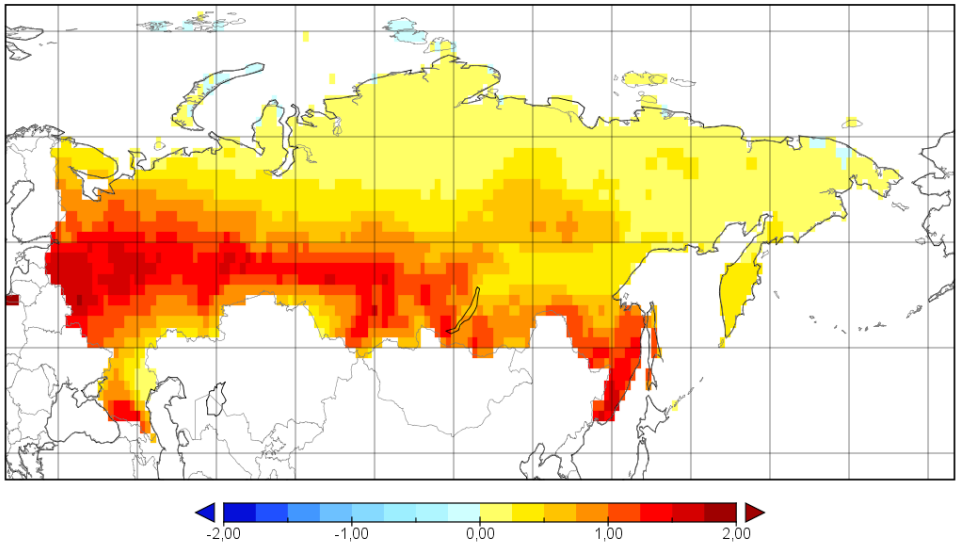

Figure 1. Ensemble mean annual uptake [μg s^{-1} m^{-2}] of carbon dioxide from the territory of Russia.

The end of the "historical" calculation period (1990-2014) was chosen for the analysis. The data from 18 models were considered, most of which had several variants with different initial conditions. Figure 1 shows the average spatial distribution of ensemble mean annual CO_2 fluxes in 1990-2014 over the ensemble of models, obtained by interpolating data from all models on a 1x1-degree grid. The main amount of carbon dioxide is absorbed on the European territory of Russia and in general in the western and southern regions of the country, excluding areas adjacent to Kazakhstan and the Caspian Sea. The net absorption of CO_2 at a rate of 0.5 - 2 μg s^{-1} m^{-2} is characteristic for almost the entire territory, except for some Arctic regions.

At the same time, the standard deviation of CO2 fluxes on the annual mean scale (Fig. 2) is generally all over Russia except for Primorsky Krai exceeding the corresponding mean with typical values of 1-2 μg s^{-1} m^{-2}. Total annual carbon dioxide uptake by Russian terrestrial ecosystems amounts to 0.37±0.38 PgC.

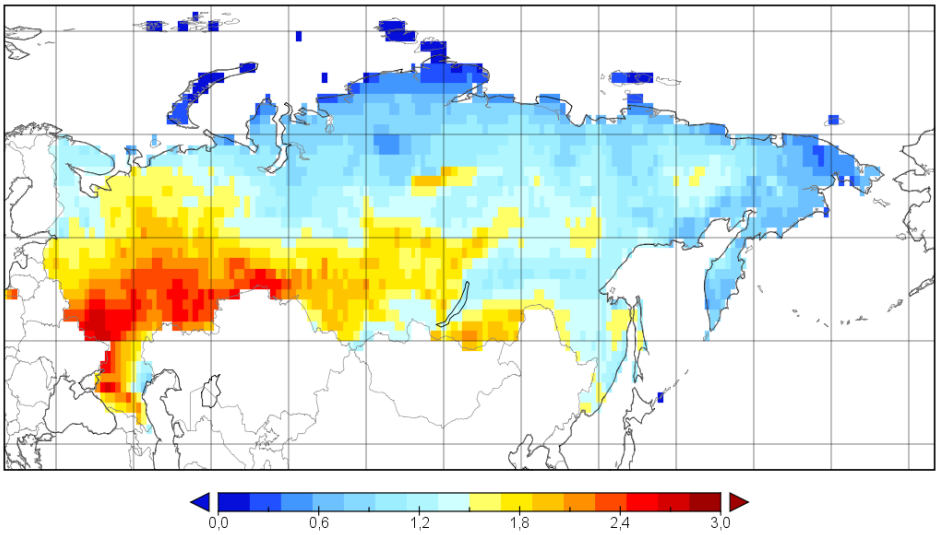

Figure 2. Standard deviation of CO_2 annual flux [μg s^{-1} m^{-2}] from the territory of Russia.

Such inter-model discrepancy can also be seen on the average monthly scale (Fig. 3). While most models show maximum CO_2 uptake in July, August and September, the BCC-CSM2-MR model and 3 models of the EC-Earth3 family show a significant decrease in uptake by this point. For the BCC-CSM2-MR model, the maximum CO_2 emission into the atmosphere is reached in the late summer and early autumn. This probably makes the BCC-CSM2-MR the only model that consistently shows negative values (-0.67 PgC on average) of CO2 uptake by terrestrial ecosystems in Russia over the considered period.

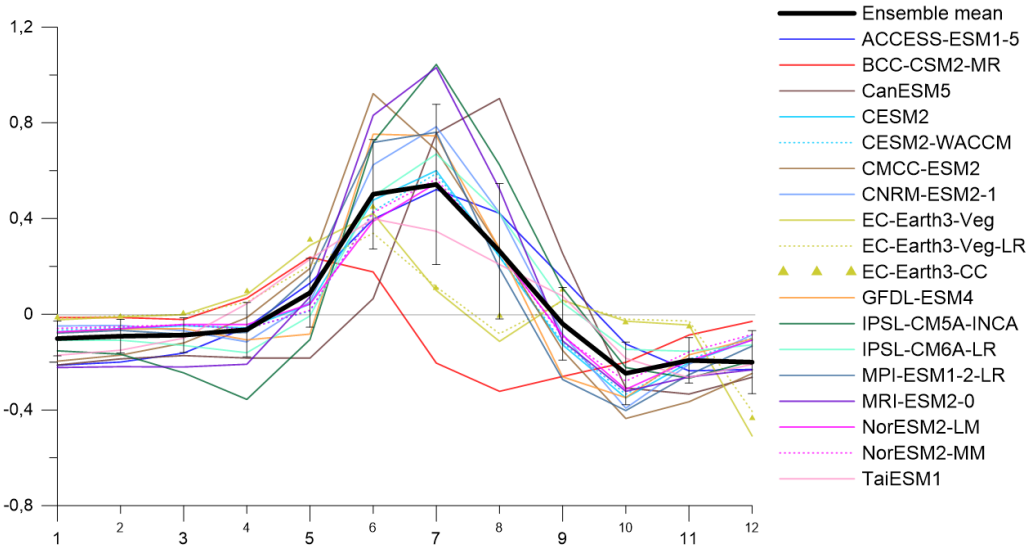

Figure 3. Monthly mean net CO_2 fluxes [PgC] from the territory of Russia simulated by CMIP6 models.

In general, although most of the models show similar behavior on an intraannual timescale, estimates of total carbon dioxide uptake on the spatial scale of even such large regions as the territory of Russia differ significantly. Net annual emission ranges from -0.67 to 0.83 PgC, whereas the individual models represent the entire range of positive values (except for BCC-CSM2-MR) and no modality is observed.

This work was supported by the Russian Science Foundation (project 19-17-00240).

1. S.N. Denisov, A.V. Eliseev, I.I. Mokhov Contribution of natural and anthropogenic emissions of CO_2 and CH_4 to the atmosphere from the territory of Russia to global climate change in the 21st century // Doklady Earth Sciences. 2019. V.488. N.1. pp. 1066–1071.

Cloud feedbacks in MRI-ESM2

Hideaki Kawai (h-kawai@mri-jma.go.jp), **Tsuyoshi Koshiro, and Seiji Yukimoto**
Meteorological Research Institute, JMA

1. Introduction

The cloud feedbacks in MRI-ESM2 (Yukimoto et al. 2019), which was used for CMIP6 simulations, are briefly investigated. Changes in the vertical profiles of cloud radiative effect (CRE), cloud cover, liquid and ice water content, and number concentrations of cloud droplets and ice crystals are examined. These profile changes are examined for several areas with typical cloud regimes to understand the contributions from each cloud regime to the global cloud feedback.

2. Model and Experiments

The model resolution is TL159L80. Averages over 36 years (1979−2014) of data from amip and amip-p4K (amip with SST increased uniformly by 4 K) runs are used for the analysis. Data from amip and amip-p4K experiments with the convection scheme switched off, which were run under the second version of the project SPOOKIE (Selected Process On/Off Klima Intercomparison Experiment; Webb et al. 2015), are also examined to understand the roles of convection schemes in the cloud feedback in MRI-ESM2.

3. Results

3.1. Overview

The cloud feedback in MRI-ESM2 for shortwave (SW) radiation is +0.27 W/m^2/K, and that for longwave (LW) is −0.17, with the sum being +0.10 W/m^2/K. As is well known, the CRE changes in LW (Fig. 1a) and SW radiation (Fig. 1b) at the top of the atmosphere (TOA) tend to cancel each other out for high-level cloud areas, and the CRE changes in the sum of SW and LW radiation (Fig. 1c) reflect the changes in SW components, especially over low-level cloud areas. In addition, high-level cloud changes (Fig. 1d) correspond well to the LW changes (Fig. 1a), and low-level cloud changes (Fig. 1f) correspond well to the SW changes (Fig. 1b).

3.2. Vertical profile analysis

To understand the CRE changes, we perform a vertical profile analysis for CRE.

We focus on the SW component in this report. The approximate CRE (W/m^2) of clouds between the surface z_0 and height z for upward SW radiation, CRE_SW↑($z - z_0$), is estimated as follows:

CRE_SW↑($z - z_0$) ≈ (SW↑(all sky, z) − SW↑(clear sky, z)),

where SW↑ denotes the upward SW radiative flux (the sign is positive for net downward; Fig. 2a). In this formula, the radiative effect of clouds between TOA and z_0 to the downward SW flux is also implicitly included. To eliminate this effect, the term −(SW↑(all sky, z_0) − SW↑(clear sky, z_0)) should be added to the right-hand side (Kawai et al. 2016). By differentiating the profiles vertically, the detailed contribution of cloud at each level to the CRE can be obtained (Fig. 2b). The contribution of clouds to SW cloud feedback can be roughly estimated from the difference between the amip-p4K and amip simulations of the profiles of the contributions to CRE_SW↑($z - z_0$) (Fig. 2c).

Figure 2c shows that the vertical profile of the contribution to the CRE change for upward SW radiation is negative at levels of 100–200, 300–500, and ~800 hPa, and positive for 750–500 and ~900 hPa.

Figure 3 shows the vertical profiles of the contribution of the CRE changes for several areas with typical cloud regimes. The global positive CRE change around 900 hPa is consistent with the positive CRE change off Peru (subtropical stratocumulus area) and near Easter Island (shallow convection area). The global negative CRE change around 800 hPa is consistent with the negative CRE change near Easter Island (shallow convection area).

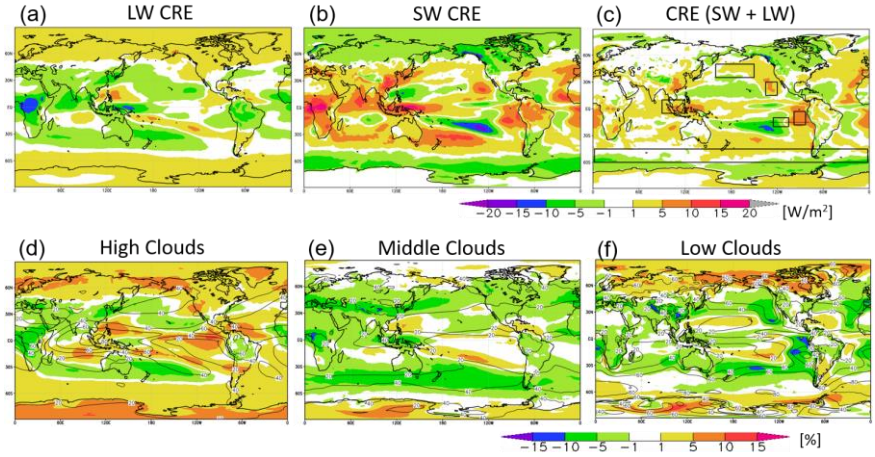

Fig. 1: Changes in CRE (amip-p4K − amip; shading) for LW (a), SW (b), and the sum of SW and LW radiation (c) at TOA, together with changes in high- (d), mid- (e), and low-level cloud cover (f). Contours are amip climatologies. MRI-ESM2 is used and the climatologies cover the period 1979–2014.

The global positive CRE change at 750–500 hPa is consistent with those near Indochina (deep convection area) and over the Southern Ocean (mid-latitude ocean). The global negative CRE change at 100–200 hPa is consistent with that near Indochina (deep convection area), and the increase in the altitude of high clouds over this region contributes to this positive CRE change. The increase in high-level clouds shown in Fig. 1d and the decrease in mid-level clouds in Fig. 1e may be partly attributed to the increase in the altitudes of high cloud layers and the cloud peak at the melting layer, and drying of the mid-level troposphere.

The noticeable reduction in the number concentration of cloud droplets and ice crystals found in MRI-CGCM3 (Kawai et al. 2015) does not occur in MRI-ESM2. The noticeable reduction in the number concentration of cloud droplets in MRI-CGCM3 was caused by a bug in the number concentration calculation.

3.3. Change in Low Clouds

Figure 1f shows that low-level clouds decrease over subtropical stratocumulus areas off the west coast of the continents. Figure 4 shows the cross-section across 15°S off Peru. Figure 4a–b clearly shows that the stratocumulus deck off Peru decreases at levels below the 850 hPa level and cumulus cloud increases above the 850 hPa level far from the coast. When the convection scheme is turned off (Fig. 4c–d), the stratocumulus deck spreads farther westward because ventilation of humidity in the boundary layer to the free atmosphere by convection does not occur. The significant reduction of the stratocumulus deck in the warmer climate is even more remarkable in the convection-off case. In MRI-ESM2, the cloud top mixing and shallow convection are suppressed when ECTEI (Estimated cloud-top entrainment index; Kawai et al. 2017) is large. Because ECTEI decreases in the future climate (Kawai et al. 2017, 2019, Koshiro et al. 2022), this parameterization may contribute to the reduction in low-level clouds in the warmer climates.

Acknowledgements

This work was partly supported by the Integrated Research Program for Advancing Climate Models (TOUGOU) Grant Number JPMXD0717935561 from the Ministry of Education, Culture, Sports, Science and Technology (MEXT), Japan. It was also supported by the Japan Society for the Promotion of Science (JSPS) KAKENHI (Grant Nos. JP18H03363, JP19K03977, and JP19H05699), and the Environmental Restoration and Conservation Agency, Japan (the Environment Research and Technology Development Fund (Grant No. 2-2003)).

References

Kawai, H., T. Koshiro, and M. J. Webb, 2017: *J. Climate*, **30**, 9119–9131.

Kawai, H., et al., 2015: *CAS/JSC WGNE Research Activities in Atmospheric and Oceanic Modelling/WMO*, **45**, 7.11-7.12.

Kawai, H., et al., 2016: *Atmos. Sci. Let.*, **17**, 548-555.

Kawai, H., et al., 2019: *Geosci. Model Dev.*, **12**, 2875–2897.

Koshiro, T., H. Kawai, and A. T. Noda, 2022: *Proc. Natl. Acad. Sci. USA*, submitted.

Webb, M. J., et al., 2015: *Phil. Trans. R. Soc. A*, **373**, 20140414.

Yukimoto, S., et al., 2019: *J. Meteor. Soc. Japan*, **97**, 931–965.

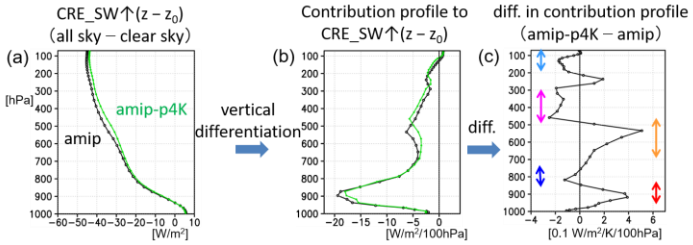

Fig. 2: (a) Cloud radiative effect (W/m^2) of clouds between the surface z_0 and height z for upward SW radiation, $\mathrm{CRE\_SW}\uparrow(z-z_0)$ (black line corresponds to amip and green line amip-p4K), (b) vertical differentiation of the profiles shown in (a) that corresponds to the contribution of cloud at each level to the CRE, and (c) the difference in the contribution profiles between the amip-p4K and amip simulations shown in (b) that is normalized by 2m temperature increase. Note that $(\mathrm{CRE\_SW}\uparrow(z_{\mathrm{TOA}})_{\mathrm{amip\text{-}p4K}} - \mathrm{CRE\_SW}\uparrow(z_{\mathrm{TOA}})_{\mathrm{amip}})/\Delta T_{2m}$ corresponds to the SW cloud feedback. Model level data are used.

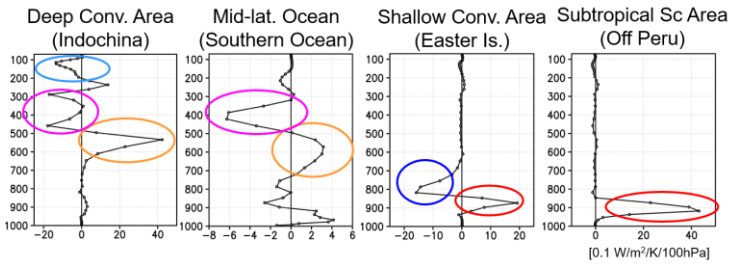

Fig. 3: Same as Fig. 2c but for the deep convection area (near Indochina), mid-latitude ocean (the Southern Ocean), shallow convection area (near Easter Island), and subtropical area (off Peru) shown in Fig.1c.

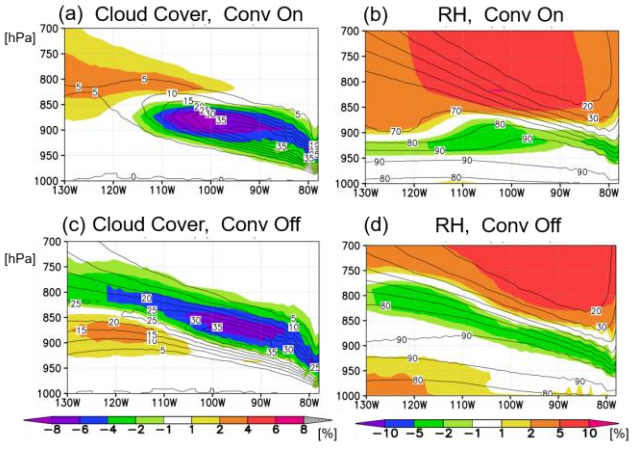

Fig. 4: Cross-sections of cloud cover (a, c) and relative humidity (b, d) along 15°S (line in Fig. 1c) (shading: difference between amip-p4K and amip; contours: amip climatology). Results of the normal model (a, b) and the convection switched off version (c, d) are shown.

Atmospheric centers of action in the Northern Hemisphere: Possible changes in the 21st century from CMIP6 model simulations

Mokhov I.I.[1,2], Osipov A.M.[2], Chernokulsky A.V.[1]

[1]A.M. Obukhov Institute of Atmospheric Physics RAS
[2]Lomonosov Moscow State University
mokhov@ifaran.ru

An analysis of possible changes of the atmospheric centers of action (ACA) in the Northern Hemisphere under global warming was carried out. We used the results of simulations with climate models of the CMIP6 ensemble with the SSP5-8.5 scenario for the 21st century.

The areas corresponding to each of the analyzed ACAs were identified similar to (Mokhov et al., 2020). Within the area corresponding to ACA, the mean sea level pressure Pc was determined with increased or decreased pressure for anticyclonic or cyclonic conditions, respectively (see also (Mokhov et al., 2018; Mokhov et al., 2021). The ACA intensity was characterized both by the pressure at sea level in the ACA region Pc and by the corresponding pressure drop Ic relative to the mean hemispheric pressure P_H at sea level. We also analyzed the relative changes in the ACA intensity Ic = Ic/ δ Ic - when normalizing Ic to the corresponding standard deviations (SD) δIc.

Table 1. Intensity Ic [hPa] of ACAs in the Northern Hemisphere for winter (a) and summer (b) from simulations with selected CMIP6 ensemble of climate models and by ERA5 reanalysis data for the base period 1981-2005. The standard deviations (SD) of the ACA intensity are given in parentheses.

(a)

ACA Seasonal Mean Intensity (hPa)	Winter (DJF)	
	Reanalysis	CMIP6 models
Azores High	4.8 (±1.6)	5.0 (±2.0)
Siberian High	10.5 (±1.1)	10.2 (±1.5)
North American High	3.0 (±1.0)	3.2 (±1.3)
Aleutian Low	-9.6 (±2.7)	-9.9 (±3.5)
Icelandic Low	-10.9 (±2.8)	-11.4 (±3.1)

(b)

ACA Seasonal Mean Intensity (hPa)	Summer (JJA)	
	Reanalysis	CMIP6 models
Azores High	8.2 (±0.6)	8.4 (±0.6)
Hawaiian High	7.6 (±0.6)	8.0 (±0.7)
Asian Low	-8.4 (±0.3)	-8.7 (±0.5)

The quality of the ACAs simulations was evaluated in comparison with ERA5 reanalysis data (https://www.ecmwf.int/en/forecasts/datasets/reanalysis-datasets/era5) for the base period 1981-2005. As a result of a comparative analysis with reanalysis data, 11 models of the CMIP6 ensemble were selected, which best reproduce the ACAs for the base period in comparison with the reanalysis data. Table 1 presents intensity Ic of key centers of atmospheric action in the Northern Hemisphere for winter (a) and summer (b) from simulations with selected CMIP6 ensemble of climate models and by ERA5 reanalysis data for the base period 1981-2005. The standard deviations (SD) of the ACA intensity are given in parentheses.

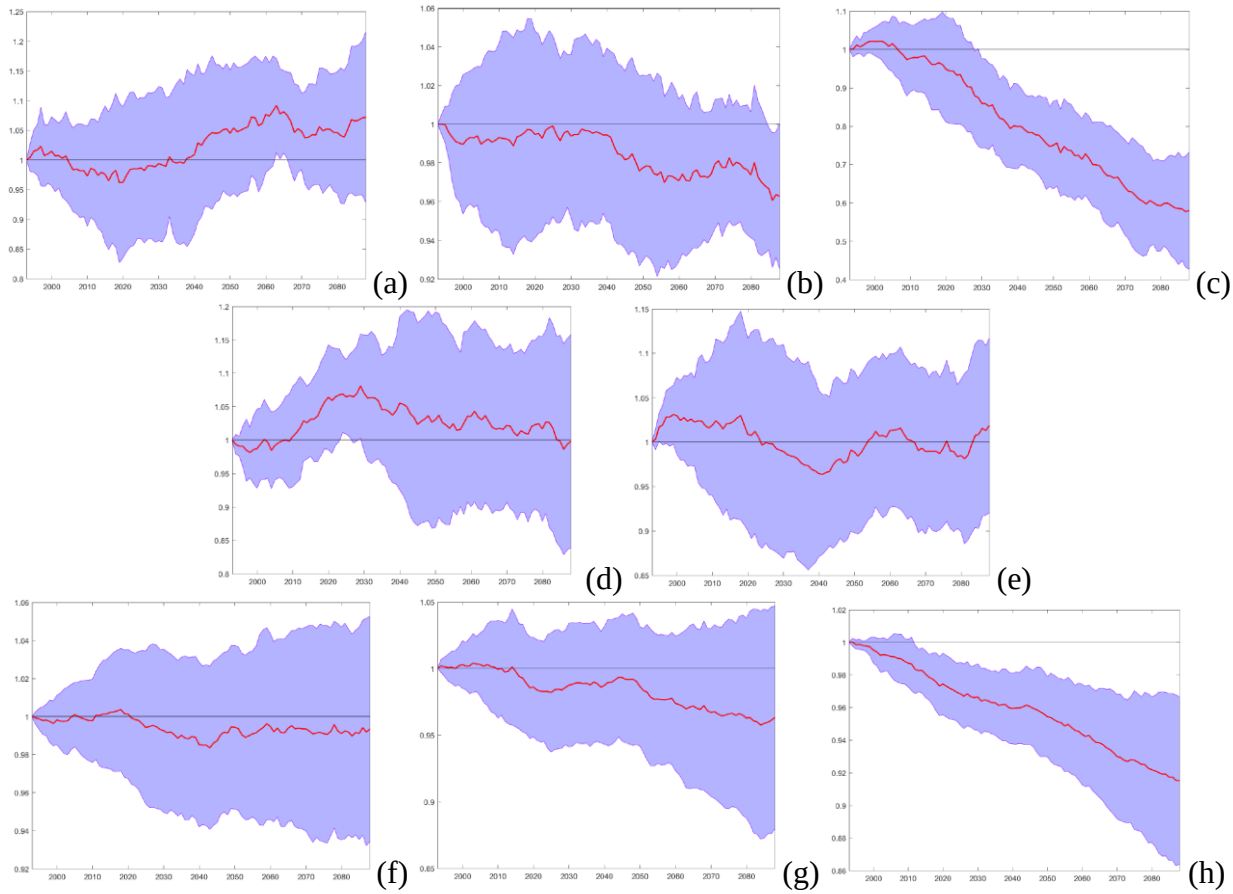

Figure 1. Changes in ACA intensity (normalized to SD for the base period 1981-2005) in the Northern Hemisphere according to simulations with a selected ensemble of CMIP6 models under the SSP5-8.5 scenario. Here: (a) Azores High, (b) Siberian High, (c) North American High, (d) Aleutian Low, (e) Icelandic Low - winter ACA; (f) Azores high, (g) Hawaiian High, (h) Asian Low – summer ACA. SD ranges relative to 30-year moving averages (red curves) are shaded.

Possible changes in the ACA intensity in the Northern Hemisphere from simulations with a selected ensemble of CMIP6 models under the SSP5-8.5 scenario for the 21st century are presented on Fig. 1. The most consistent estimates based on simulations with the ensemble of the CMIP6 models were obtained for the weakening tendencies of the winter North American High and the summer Asian Low. For the Siberian High in winter, the weakening trend was found less significant.

This work was supported be the Russian Science Foundation (project 19-17-00240).

References

Mokhov I.I., Chernokulsky A.V., Osipov A.M. Changes in the characteristics of atmospheric centers of action. In: Intense Atmospheric Vortices and Their Dynamics. Ed. By I.I. Mokhov, M.V. Kurgansky, O.G. Chkhetiani. Moscow, GEOS, 2018, 398—403. (In Russian)

Mokhov I.I., Chernokulsky A.V., Osipov A.M. Atmospheric centers of action in the Northern and Southern Hemispheres: Features and variability. Rus. Meteorol. Hydrol., 2020, V. 45, No. 10, pp. 749–761.

Mokhov I.I., Chernokulsky A.V., Osipov A.M. Atmospheric centers of action in the Northern and Southern Hemispheres: Tendencies of change in the 21st century from model simulations. Research Activities in Earth System Modelling. 2021. Rep. 51. WCRP Report No.4/2021. WMO, Geneva, S. 7. P. 11-12.

Determining the cause-effect relationship between climatic variables based on time series: is it possible or not?

Muryshev K.E.[1,2], Eliseev A.V.[1,2], Mokhov I.I.[1,2], Timazhev A.V.[2]

[1] Lomonosov Moscow State University

[2] A.M. Obukhov Institute of Atmospheric Physics? Russian Academy of Sciences

kmuryshev@mail.ru

According to paleoreconstructions and observational data for the late XX – early XXI centuries, it is noted that time series for global temperature T are generally leading the corresponding time series for the CO_2 content in the atmosphere q (references to the relevant works are given in [1, 2]). On this basis, it is sometimes stated that the modern theory of global warming, according to which the main reason for the ongoing increase in global temperature is CO_2 emissions into the atmosphere, is incorrect. These statements are made without involving any ideas about the structure of the Earth's system, but only on the basis that the "effect" (temperature) cannot lead the "cause" (CO_2).

The lag of q changes relative to T changes is also obtained in simulations with modern climate models (in particular, with the MPI-ESM general circulation model included in the CMIP-6 model comparison project, see fig. 1), in which the CO_2 greenhouse effect is the main cause of the ongoing global warming.

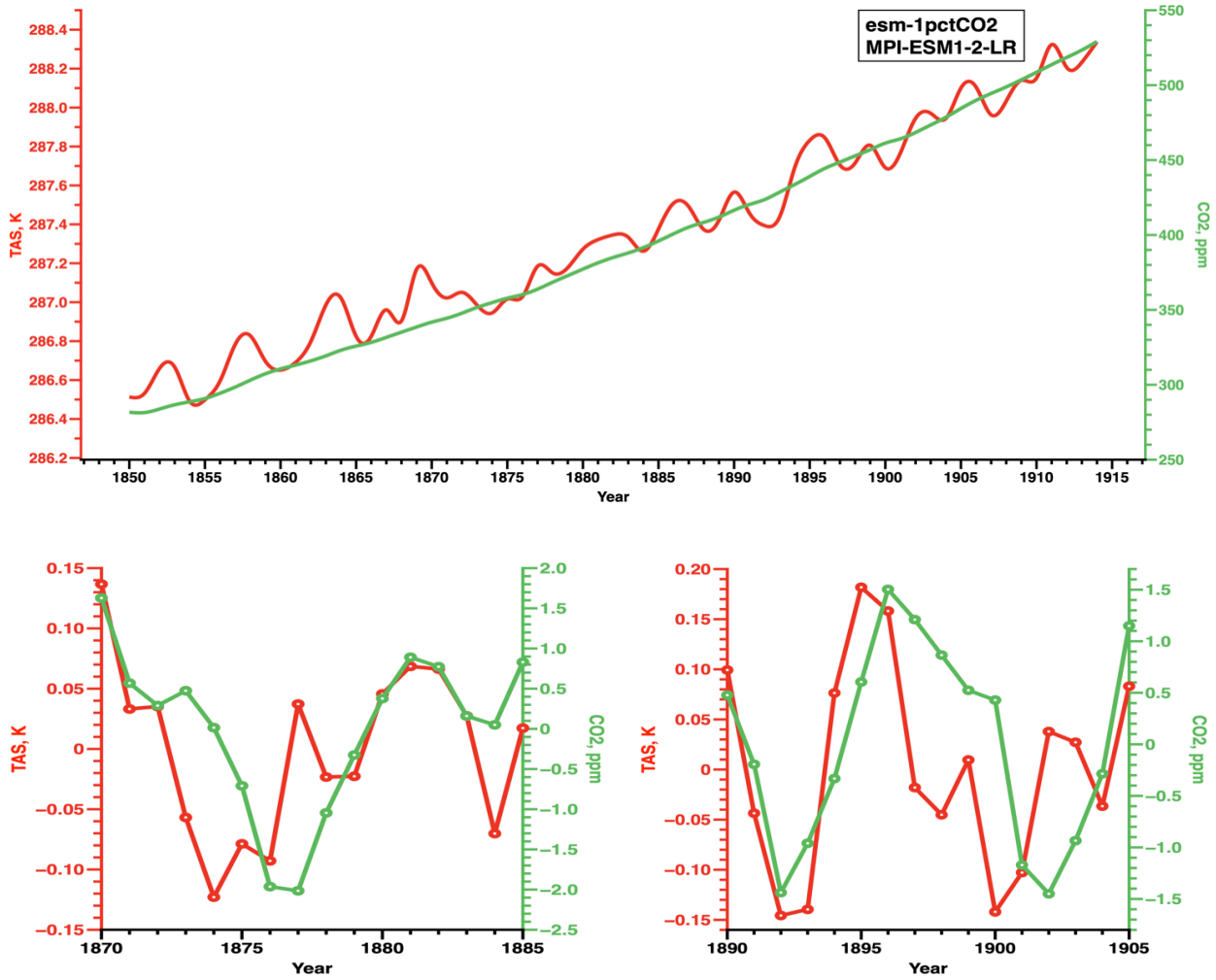

Fig. 1. Changes in global temperature (red) and CO_2 content in the atmosphere (green) in simulations with the MPI-ESM climate model. The upper part of the figure shows the initial series, the lower part shows the series with the linear trend removed.

This result illustrates the fact that time lag between changes in variables cannot be used to judge the nature of the causal relationship between them. Moreover, not only the time lag between the series, but also any other characteristics of these series do not allow us to draw a final conclusion about the nature of the causal relationship between the corresponding variables, without any ideas about the nature of the interaction of these variables or, to put it more formally, about the structure of the system in which they are exist. Let's show it.

Consider two arbitrary data series from a finite number of *n* elements:

$$X = [\, x_1, \ \dots, x_n \,], \quad (1)$$

$$Y = [\, y_1, \ \dots, y_n \,]. \quad (2)$$

If the values of all their elements are limited (this is always valid for real data series) and are non-zero (this can be achieved by choosing measurement units), then it is possible to build a system where changes in *X* are the cause of changes in *Y*, that is, changes in *X* affect changes in *Y*, and changes in *Y* do not affect changes in *X*. In the simplest case, this can be written as a differential equation:

$$\frac{dY}{dt} = f(X, t). \quad (3)$$

Here *f* is some arbitrary function, *t* is time. Let function f be linear:

$$f(X, t) = K(t)X(t). \quad (4)$$

Taking into account (3) and (4), we obtain

$$K(t) = \frac{Y'(t)}{X(t)}. \quad (5)$$

Then, using (1) and (2), it is possible to obtain a number of specific values of *K* corresponding to the original series *X* and *Y*:

$$K_n = (y_{n+1} - y_n) / (x_n \Delta t). \quad (6)$$

Here Δt is a time step. Thus, the system follows

$$y_{n+1} = K_n x_n \Delta t + y_n. \quad (7)$$

Within this system, changes in *X* are the cause of changes in *Y*. Since the series were taken arbitrarily, in a similar way it is possible for the same series to construct a system in which, on the contrary, changes in *Y* will cause changes in *X*.

Thus, for any pair of series *X*, *Y*, whose values are nonzero and limited, it is possible to construct both a system in which *Y* is the cause and *X* is the effect, and vice versa. This means that on the base of data series analysis only, it is impossible to draw an unambiguous conclusion about the nature of the causal relationship between their changes, without assuming a physical theory of their interaction.

This work was supported by the Russian Science Foundation (project 19-17-00240).

References:

1. *Muryshev K.E., Eliseev A.V., Mokhov I.I., Timazhev A.V.* Lead-lag relationships between global mean temperature and and the atmospheric CO_2 content in dependence of the type and time scale of the forcing. *Global and Planetary Change,* 2017, V. 148, P. 29–41.
2. *Muryshev K.E., Eliseev A.V., Mokhov I.I., Timazhev A.V., Arzhanov M.M., Denisov S.N.* Influence of Nonlinear Processes on the Time Lag between Changes in the Global Temperature and the Carbon Dioxide Content in the Atmosphere. *Dokl. Earth Sci.*, 2021, V. 501, P. 949–954.